

Modelling the compliance of crustal rock—II. Response to temporal changes before earthquakes

Stuart Crampin* and Sergei V. Zatsepin

Department of Geology and Geophysics, University of Edinburgh, Grant Institute, West Mains Road, Edinburgh EH9 3JW, UK.
E-mail: scrampin@ed.ac.uk; zats@glg.ed.ac.uk

Accepted 1996 October 16. Received 1996 July 25; in original form 1995 August 18

SUMMARY

There have been several claims that seismic shear waves respond to changes in stress before earthquakes. The companion paper develops a stress-sensitive model (APE) for the behaviour of low-porosity low-permeability crystalline rocks containing pervasive distributions of fluid-filled intergranular microcracks, and this paper uses APE to model the behaviour before earthquakes. Modelling with APE shows that the microgeometry and statistics of distributions of such fluid-filled microcracks respond almost immediately to changes in stress, and that the behaviour can be monitored by analysing seismic shear-wave splitting. The physical reasons for the coupling between shear-wave splitting and differential stress are discussed.

In this paper, we extend the model by using percolation theory to show that large crack densities are limited at the grain-scale level by the percolation threshold at which interacting crack clusters lead to pronounced increases in rock-matrix permeability. In the simplest formulation, the modelling is dimensionless and almost entirely constrained without free parameters. Nevertheless, APE modelling of the evolution of fluid-saturated rocks under stress reproduces the observed fracture criticality and the narrow range of shear-wave azimuthal anisotropy in crustal rocks. It also reproduces the behaviour of temporal variations in shear-wave splitting observed before and after the 1986, $M=6$, North Palm Springs earthquake, Southern California, and several other smaller earthquakes.

The agreement of APE modelling with a wide range of observations confirms that fluid-saturated crystalline rocks are stress-sensitive and respond to changes in stress by critical fluid-rock interactions at the microscale level. This means that the effects of changes in stress and other parameters can be numerically modelled and monitored by appropriate observations of seismic shear waves.

Key words: earthquakes, fractures, shear-wave splitting, stress distribution, temporal changes.

The earth hath bubbles, as the water has,
And these are of them.
(Shakespeare 1623)

1 INTRODUCTION

The critical role of fluid-filled inclusions in impending catastrophes has been recognized for over 350 years. There have been several more recent claims that the seismic response, specifically the time delay between split shear waves in low-permeability low-porosity igneous and metamorphic crystalline

rocks, varies before earthquakes, and during hydraulic pumping. These effects have been interpreted as the seismic response to stress-induced changes in the geometry of distributions of closely spaced fluid-filled microcracks and intergranular pore space, known as *extensive-dilatancy anisotropy* or *EDA* (Crampin, Evans & Atkinson 1984). Crampin (1994) reviewed data suggesting that EDA cracks are pervasive throughout almost all rocks in the crust. In the companion paper, Zatsepin & Crampin (1997), hereafter referred to as Paper I, we show that low-permeability low-porosity crystalline rocks containing fluid-filled *intergranular* EDA cracks are necessarily compliant to small changes in differential stress. Paper I shows that microcrack geometry in low-permeability low-porosity rocks responds almost immediately to changes in stress by fluid

* Also at: Edinburgh Anisotropy Project, British Geological Survey, Murchison House, West Mains Road, Edinburgh EH9 3LA, UK.

diffusive mass transfer (and by fluid flow in porous rocks) along pressure gradients between closely spaced fluid-filled intergranular EDA cracks at different orientations to the stress field. Numerical modelling based on an anisotropic poroelasticity (APE) model (Paper I) of the behaviour of pre-stressed fluid-saturated rock shows that such fluid-filled inclusions necessarily become aligned when subjected to differential stress and display the observed seismic anisotropy.

In this paper, we use APE to model temporal changes in shear-wave splitting in response to changes in differential stress. The concept of fracture criticality (Crampin 1994) and simple estimates based on percolation theory (Kirkpatrick 1973; Dienes 1982) restrict the value of effective crack density to yield the narrow range of shear-wave velocity anisotropy observed in the crust.

A remarkable feature of APE modelling is that, in the simple formulation for low-permeability low-porosity rocks (Paper I), the model is dimensionless and without free model parameters, yet it reproduces, without adjustment and with few assumptions, the observed characteristics of shear-wave splitting, including the behaviour before and after earthquakes. The close relationship between the fracture criticality of fluid-saturated rocks at the microscale level and self-organized criticality of crustal rocks displayed in different scale-invariant geological structures is discussed. We show that the observed behaviour of shear-wave splitting is evidence of the proximity of fracture criticality (and metastability) in pre-stressed fluid-saturated crustal rocks. This has important consequences for monitoring stress before earthquakes, as well as a wide range of other geological and industrial applications.

The terminology for anisotropy used in this paper is that suggested by Crampin (1989). The notation is listed in Appendix A of Paper I.

2 SHEAR-WAVE SPLITTING AND TEMPORAL VARIATIONS

Shear-wave splitting, where the polarizations of the faster phase are subparallel to the direction of maximum horizontal stress, was first positively identified in crustal rocks above earthquakes during the three Turkish Dilatancy Projects [TDP1: Crampin *et al.* (1980); TDP2: six papers, beginning with Crampin, Evans & Üçer (1985); and TDP3: three papers beginning with Evans *et al.* (1987)]. The splitting was attributed to propagation through distributions of near-parallel near-vertical EDA cracks. Shear-wave splitting has also been observed in exploration seismics in sedimentary basins (Crampin 1984a; Crampin *et al.* 1986), and at the meeting of the Society of Exploration Geophysicists in Houston, 1986, several oil companies reported shear-wave splitting (including Alford 1986; Willis, Rethford & Bielandski 1986). Since 1980, shear-wave splitting has been widely observed in almost all types of igneous, metamorphic, and sedimentary rocks, in almost all types of tectonic and geological conditions (see reviews by Crampin 1987 and Crampin 1994).

[Note that earlier observations of shear-wave splitting in the crust (Byerly 1938; Gupta 1973) were recorded well outside the shear-wave window (Booth & Crampin 1985). This makes them difficult, if not impossible, to interpret directly in terms of crustal anisotropy (Crampin *et al.* 1981).]

Temporal variations in traveltimes of *P* and *S* waves have occasionally been observed before large earthquakes (Semenov

1969; Whitcomb, Garmany & Anderson 1973; and others), and before the larger events in isolated swarms of small-magnitude earthquakes (Aggarwal *et al.* 1973; Chiu *et al.* 1984). It was suggested (Nur 1972; Aggarwal *et al.* 1975), as we now think correctly, that such temporal variations were caused by the movement of fluids during stress-induced modifications of microcrack geometry in the dilatancy fluid-diffusion hypothesis. At that time, however, such dilatancy was thought to require the migration of fluids over substantial distances in short periods of time, which was clearly unlikely. Consequently, dilatancy was rejected, particularly as, despite careful analyses of traveltimes before large earthquakes, changes in velocities were not consistently observed.

Crampin (1978) showed that such stress-induced modifications would necessarily lead to stress-aligned microcracks and effective seismic anisotropy. Consequently, changes in body-wave velocities would only be expected for particular source and receiver geometries depending on the focal mechanism, the orientations of the stress field, and the locations of the earthquakes.

Temporal variations in the time delays between split shear waves have been reported before and after the $M=6$, North Palm Springs earthquake of 1986 July 8 in Southern California (Crampin *et al.* 1990, 1991), before and after a smaller earthquake in Arkansas (Booth *et al.* 1990), Parkfield (Liu *et al.* 1993; Liu 1995) and (two earthquakes) on Hainan Island, China (Gao *et al.* 1997). These temporal variations show patterns of changes varying with the direction of propagation. The three-dimensional pattern of variations in time delays could be simulated (Peacock, Crampin & Booth 1988; Crampin *et al.* 1990, 1991) by increasing the aspect ratios of aligned EDA cracks before the earthquakes, and decreasing the aspect ratios to the initial values shortly after the earthquake (or in one case immediately before the earthquake; Booth *et al.* 1990). The observations of the North Palm Springs earthquake were disputed by Aster, Shearer & Berger (1990, 1991), but their arguments can be discounted as their results were based on an automatic technique to read shear-wave time delays that was demonstrably inadequate with errors of 200 per cent (Crampin *et al.* 1991).

Note that it is difficult to monitor shear-wave splitting before earthquakes because of the constraints on recording geometry. Identifying changes of splitting before large earthquakes requires suitable three-component seismic networks with high digital sampling rates sited within the preparation zone of impending larger earthquakes. Since the build-up of deformation before a large earthquake may occur over many millions of cubic kilometres, this may not be a serious restriction. However, a more severe requirement is the need for sufficient small earthquakes within the shear-wave window beneath the network stations to provide shear-wave sources in order to obtain reliable data on the temporal variations of time delays between split shear waves over a wide solid angle of directions. These constraints are severe and have, to our knowledge, only been met (serendipitously) in the four areas identified above, which in all cases displayed temporal changes. There are to our knowledge no contrary observations.

Identifying changes in shear-wave splitting (or any other precursory phenomena) before larger 'typical' events in *isolated swarms* of earthquakes, a long way from other seismic activity, may be particularly valuable (Crampin 1991, 1993). The study of such isolated swarms is informative as precursory

phenomena may be seen before typical events, which repeat frequently, sometimes every few days. Isolated swarms are rare, and such studies have only been possible [other than at Blue Mountain Lake, New York (Aggarwal *et al.* 1973, 1975)], at Enola, Arkansas (Booth *et al.* 1990) and Hainan Island, China (Gao *et al.* 1997)], as they are difficult to recognize and instrument in the comparatively short time that they are active. Again serendipity must be invoked!

Changes in shear-wave splitting have also been identified during a hydraulic fracture experiment in the Lost Hills Oil Field, California (Meadows & Winterstein 1994). These were modelled in detail (Meadows & Winterstein 1994; Liu, Crampin & Hudson 1997). More subtle changes in shear-wave splitting have also been observed in the hot-dry-rock geothermal experiment at the Camborne School of Mines, Cornwall while testing hydraulic pumping equipment (Crampin & Booth 1989).

3 SHEAR-WAVE SPLITTING, FRACTURE CRITICALITY, AND THE PERCOLATION THRESHOLD

3.1 Observations of shear-wave splitting

Reviewing available publications, Crampin (1994) found shear-wave splitting reported in almost all types of rocks in the upper half of the crust. Crampin analysed all (46) published observations of short-period shear waves where sufficient information was reported to quantify the anisotropy. Half of these reports were of observations in crystalline rocks above earthquakes and half from industrial controlled-source studies in sedimentary basins. The range of percentage shear-wave velocity anisotropy in ostensibly intact unfractured *in situ* rock below 1 km depth was found to be 1.5–4.5 per cent, independent of rock type (igneous, metamorphic or sedimentary). These percentages are equivalent to inferred effective crack densities $0.015 \leq \varepsilon \leq 0.045$. This percentage rises to 10 per cent ($\varepsilon \approx 0.1$) or greater near the surface, and in anomalous regions such as subduction zones, fault zones, regions of high heat flow, and specifically heavily fractured layers (Crampin 1994). The only rocks where stress-aligned azimuthal shear-wave splitting is not observed are some clays and shales, where pore fluids are tied to grain boundaries by chemical and electrical potentials, slates with dominant lithological anisotropy, and some carbonates with bizarre microstructures such as oolites.

The dimensionless crack density is usually written as $\varepsilon = na^3/v$, where n is the number of cracks of radius a in volume v (Hudson 1981), and may be specified equivalently as $\varepsilon = a^3/L^3$, where the cube of crack radius is normalized by the volume containing one crack L^3 , where L is the characteristic crack spacing. This notation allows distributions of equally sized cracks to be imaged, and the values of inferred crack density indicate closely spaced distributions of cracks. Even at the lowest observed anisotropy of 1.5 per cent, the average crack spacing is only about twice a crack diameter, and a factor of less than two in average crack spacing separates the 1.5 per cent minimum anisotropy in intact rocks ($L \approx 4a$) from the 10 per cent anisotropy ($L \approx 2a$) observed in heavily fractured disaggregated near-surface rocks (Crampin 1994).

3.2 Fracture criticality

The narrow range of shear-wave splitting observed in ostensibly intact rock implies pervasive crack distributions with the crack density restricted by some critical phenomenon: the *fracture criticality* of fluid-saturated crustal rocks (Crampin 1994). Crampin suggested that the value of crack density in such pervasive crack distributions is limited by pronounced increases in rock-matrix permeability caused by interacting cracks, so that pore fluids disperse and the crack distributions relax to a lower crack density. On the other hand, when pore fluid pressure is less than the least principal stress, the closure of pore space and various dehydration reactions tend to raise pore fluid pressure (Brodie & Rutter 1985) so that high pore fluid pressures are typical throughout crustal rocks (Neuzil 1995). As a consequence, a dynamic finely tuned metastable equilibrium of fluid-rock interactions or *fracture criticality* must be expected (Paper I).

Consequently, the existence of critical or subcritical EDA crack distributions must be expected for a rock mass containing free (not chemically or electrically bonded) pore fluids even for very low porosity. Microcracks are pervasive throughout crustal rocks (Simmons & Richter 1976; Kranz 1983), and the presence of free fluids at high pore fluid pressures (Neuzil 1995) in intergranular cracks or pores with volume concentrations of at least $\phi \approx 0.1$ per cent is typical of low-permeability crystalline rocks in the upper crust (Fyfe, Price & Thompson 1978).

The concept of *fracture criticality* is based on the assumption that pore fluids disperse whenever the crack density is large enough to create a subnetwork of crack clusters with enhanced permeability. As we will show, the observed narrow range of shear-wave anisotropy follows inevitably from the assumption that the crack density is restricted by the percolation threshold for uniform spatial crack distributions.

3.3 Percolation threshold

Following Dienes (1982) and Gueguen & Dienes (1989), we consider a spatially uniform distribution of equally sized cracks with random orientations (Paper I). Fig. 1 shows the

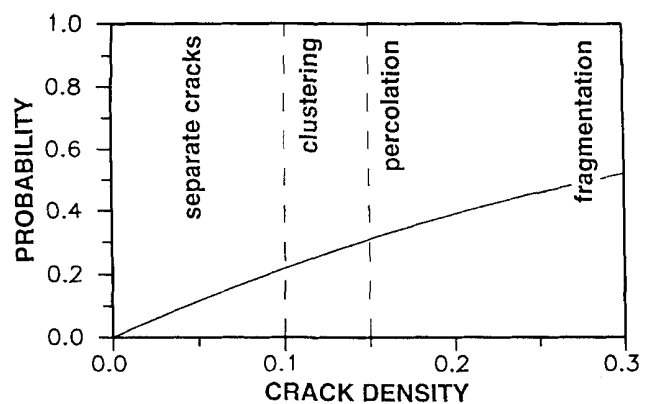


Figure 1. Probability of intersection of uniformly distributed randomly oriented equally sized cracks as a function of dimensionless crack density ε with the range of different spatial characteristics identified.

probability of cracks intersecting, given by

$$P = 1 - \exp[-(\pi/2)^2 \varepsilon], \quad (3.1)$$

where we have written the probability of cracks intersecting as a function of the dimensionless crack density ε .

For the moment, ignoring the dynamics of fluid–rock interactions in interpreting (3.1), the effective crack densities correspond to different types of spatial crack statistics. For $\varepsilon \leq 0.1$, the probability of crack intersection $P(\varepsilon)$, given by (3.1), is less than 1/4, and the crack distribution consists principally of isolated cracks. In the narrow range of crack densities below the percolation threshold ε_p , there is intensive crack intersection (crack clustering), resulting in an infinite (percolating) crack cluster at $\varepsilon = \varepsilon_p$. The percolation threshold ε_p has been evaluated for different crack statistics and usually falls in the range $0.1 \leq \varepsilon_p \leq 0.2$ (see review by Lee & Farmer 1993). We take $\varepsilon_p = 0.15$ in the middle of this range, close to the value predicted by Gueguen & Dienes (1989), where the percolation threshold occurs for the crack intersection probability $P(\varepsilon_p) = P_p = 1/3$. When $\varepsilon > \varepsilon_p$, through-going fractures exist and crack distributions become permeable for pore fluids. However, the individual elements of the rock mass remain intact up to some critical crack density ε_f , the *fragmentation threshold*. When crack density reaches this threshold, the rock is heavily fractured and fragmented and close to disaggregation, and can no longer be treated as an intact solid. The value of the fragmentation threshold is not well established (Chelidze 1982, 1986) and the region of fragmentation in Fig. 1 is presented only schematically. Note that it is not useful to discuss the ‘correct’ value for the percolation threshold at the grain-scale level, as the threshold depends on the complex geometry of pore space. In this situation, $\varepsilon_p \approx 0.15$ can be considered as a more or less reliable approximation for the value of the percolation threshold.

To show that the effect of crack clustering is large enough to promote pore fluid dispersion, we first need to estimate crack-induced permeability for clustering cracks. The specific permeability k_{cr} of spatially uniform distributions of equally sized cracks just above the percolation threshold has been calculated by Dienes (1982), and can also be presented in terms of the dimensionless crack density ε :

$$k_{cr} = 4(\pi/15)fg^3\varepsilon a^2, \quad (3.2)$$

where $f \approx 54(P - P_p)^2$ is the *percolation frequency*, the fraction of connected cracks, calculated by Gueguen & Dienes (1989) using a four-coordinate Bethe lattice, and g is the crack aspect ratio. Substituting the crack intersection probability P from eq. (3.1) into (3.2), the increase in specific permeability caused by percolation can be written

$$k_{cr} \approx 54(4\pi/15)(\pi/2)^4 (\varepsilon - \varepsilon_p)^2 g^3 \varepsilon a^2 \quad (3.3)$$

for $\varepsilon \geq \varepsilon_p$.

Note that the *infinite crack cluster permeability* given by (3.3) is a geometrical function of crack distribution variables g , ε , and a , and is without any reference to the physical or mineralogical properties or stress state of *in situ* rock. Consequently, it does not take into account the background permeability caused by other permeable (interconnected) microstructural elements. In the range $\varepsilon \leq \varepsilon_p$, the *background permeability*, k_o , of low-permeability intact rocks such as granites may be caused by a pipe network of intergranular microtubes with high connectivity, or by a mixed structure of

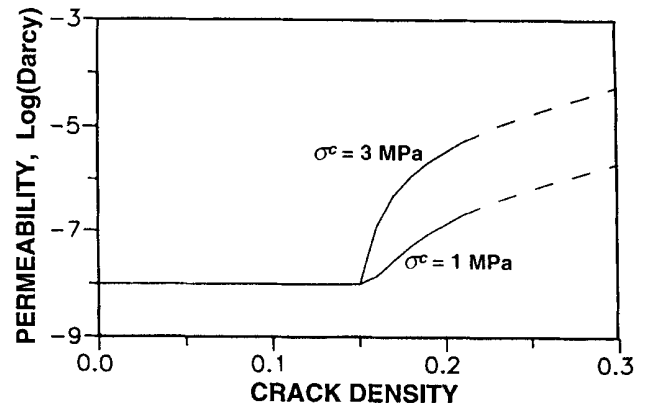


Figure 2. Increases in rock-matrix permeability of uniformly distributed randomly oriented cracks caused by percolation of crack/clusters as a function of dimensionless crack density ε for two values of aspect ratio. Crack radius is taken as 1 mm.

separate cracks connected by intergranular tubes (Géraud 1994), and is an approximately constant, slowly increasing function of crack density. As a first approximation, the total *specific microscale permeability* k_s can be written as a sum of the background permeability k_o and a crack cluster permeability k_{cr} given by (3.3), where $k_s = k_o + k_{cr}$.

Fig. 2 shows the possible behaviour of specific permeability k_s as a function of crack density for intact low-permeability rocks with an initial background permeability of $k_o = 10$ nanodarcy (10^{-20} m^2) for two values of aspect ratio. When crack density reaches and exceeds the critical percolation threshold ε_p , permeability increases abruptly by some orders of magnitude due to interconnected crack clusters. Such increasing micro-scale permeability induced by cracking above the *fracture criticality* limit was suggested by Crampin (1994) to explain the observed range of seismic azimuthal anisotropy in ostensibly intact rock. Consequently, the crack density limit of fracture criticality, ε_c , can be associated with the percolation threshold, so that $\varepsilon_c \approx \varepsilon_p$.

Consider the values of stress-induced seismic anisotropy that can be expected from an initially isotropic randomly oriented subcritical crack distribution with some crack density ε_c just below the percolation threshold. As shown in Paper I, azimuthally isotropic subvertical crack distributions are an inevitable result of a distribution of initially randomly oriented cracks, subjected to the differential stress of the vertical overburden $\Delta\sigma_v = \sigma_v - \sigma_h > 3/2\sigma^c$. The critical stress σ^c was introduced in Paper I as the inverse of the crack-space compressibility c_{cr} and is directly related to the crack aspect ratio g for the simple case of equally sized cracks. In this case the effective crack density of subvertical (azimuthally isotropic) crack distributions is given in Section 4 of Paper I as

$$\varepsilon_v = \varepsilon_c \cos\psi_o = \varepsilon_c (2s_v/3)^{-1/3}, \quad (3.4)$$

where ψ_o is the orientation angle between the crack normal and the vertical axis, separating the open crack system from closed cracks transparent to propagating seismic waves, and s_v is the normalized dimensionless differential vertical stress $s_v = \Delta\sigma_v/\sigma^c$, taken to be positive for compressional vertical differential stress (details in Section 5 of Paper I).

Fig. 3 shows the evolution of effective (normalized) crack density and angle ψ_o with increasing uniaxial loading. For a

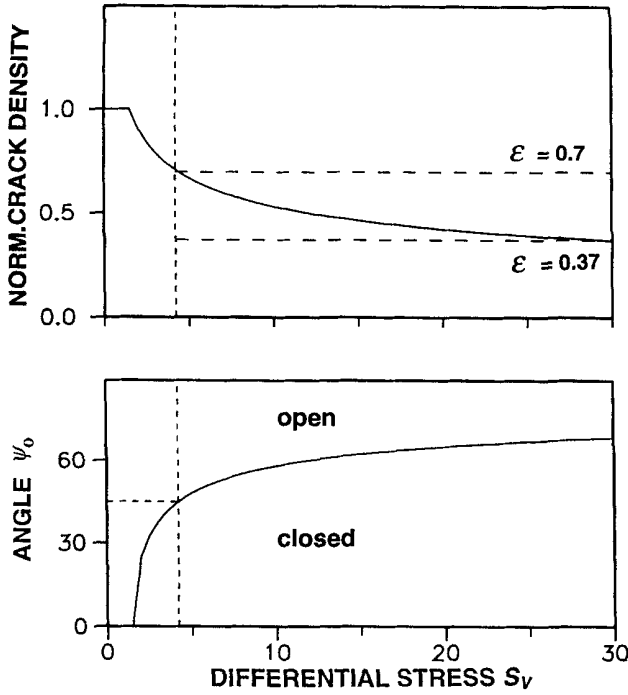


Figure 3. Upper diagram: evolution of normalized effective crack density $\varepsilon_v/\varepsilon_{v_0}$ from an initially randomly oriented crack distribution as a function of vertical differential stress, where $\varepsilon_{v_0} = \varepsilon_v$ ($s_v = 0$). The horizontal dashed lines mark the range of crack densities of near-vertically aligned cracks in the evolution of an initially randomly aligned distribution of EDA cracks subjected to increasing vertical differential stress, $0 \leq s_v \leq 30$. Lower diagram: evolution of angle ψ_0 separating open cracks from closed cracks for increasing vertical differential stress in a randomly oriented crack distribution. The horizontal dashed line separates more nearly vertically aligned cracks from more nearly horizontally aligned cracks.

vertical differential overburden stress $s_v \geq 4.2$ ($\sigma_v \geq 4.2\sigma^c$ for unnormalized dimensional stress), all subhorizontal cracks with normals oriented closer than 45° to the vertical axis are closed so that the crack distribution consists mainly of subvertical cracks. Eq. (3.4) shows that, because of the exponent $-1/3$, once the differential overburden exceeds $s_v = 4.2$, the effective crack density is rather insensitive to overburden. Fig. 3 shows that for a wide range of dimensionless (normalized) differential vertical stress, $4.2 \leq s_v \leq 30$, consistent with the strength-bearing capacity of rocks of the upper crust, effective crack density changes only within the comparatively narrow limits $0.4\varepsilon_c \leq \varepsilon_v \leq 0.7\varepsilon_c$. That is, $\varepsilon_v \approx (0.55 \pm 0.15)\varepsilon_c$ for all expected differential vertical stress components.

In the presence of horizontal differential stress, subvertical crack distributions will display seismic azimuthal EDA anisotropy due to the differential closing of the subvertical intergranular cracks relative to the principal axes of the horizontal stress field. The behaviour of effective crack density and horizontal closure angle θ_0 (see Section 5 of Paper I) almost exactly repeats the previous scenario for subvertical effective crack density ε_v and angle ψ_0 . This results in another abrupt drop in effective crack density with little further evolution for increasing differential horizontal stress in the range of the values for the normalized crack density $\varepsilon \approx (0.55 \pm 0.15)\varepsilon_v$, where $\varepsilon_v \approx (0.55 \pm 0.15)\varepsilon_c$. The total range of expected effective

crack densities for azimuthally anisotropic crack distribution is thus $\varepsilon \approx (0.55 \pm 0.15)(0.55 \pm 0.15)\varepsilon_c$, approximately $0.15\text{--}0.5\varepsilon_c$. For the subcritical crack density ε_c just below the percolation threshold $\varepsilon_c \approx 0.14$, say, the range of effective crack densities for azimuthally anisotropic crack distributions is approximately $0.02 \leq \varepsilon \leq 0.07$ for a wide range of expected differential stresses in crustal rocks.

The magnitude of shear-wave splitting for near-vertically propagated shear waves can be estimated for parallel vertical cracks in a simple form:

$$\Delta V/V = \varepsilon \Lambda, \quad (3.5)$$

where $\Delta V/V$ is the difference in the velocities of the two split shear waves normalized by the velocity of the faster wave V and $\Lambda = (8/3)(\lambda + 2\mu)/(3\lambda + 4\mu)$ is a dimensionless combination of the Lamé constants λ and μ (Crampin, 1984b). For $\lambda \approx \mu$ (Poisson's ratio ≈ 0.25), $\Lambda = 8/7 \approx 1$ and the percentage of shear-wave splitting is approximately equal to the crack density ε [see also eq. (4.1) below]. This approximation was used by Crampin (1994) to formulate the concept of fracture criticality. As follows from eq. (3.5), the expected value of azimuthal anisotropy for effective crack densities in the range $0.02 \leq \varepsilon \leq 0.07$ is a shear-wave velocity anisotropy of about 2–7 per cent. However, eq. (3.5) assumes parallel cracks. Stress-aligned cracks with a distribution of orientations lead to the lower values of shear-wave anisotropy for the given range of effective crack densities, $0.02 \leq \varepsilon \leq 0.07$. More accurate numerical calculations for distributed crack orientations give the expected percentage of stress-induced shear-wave anisotropy in the range about 1–5 per cent. The remarkable agreement with observed values of 1.5–4.5 per cent (Crampin 1994) suggests that the above analysis is appropriate for *in situ* rocks in the crust.

3.4 Fracture criticality and scale-invariant distributions of fractures

Although subcritical crack density ε_c , just below the percolation threshold $\varepsilon_p \approx 0.15$, cannot be obtained directly from seismic field data, this subcritical crack distribution is not a theoretical artefact or a purely theoretical construction. On the intergranular microscale level with a characteristic crack size of the order of grain size, the stress field affecting microcracks can be considered as the sum of the average applied stress field σ_a (local, regional and tectonic) and the perturbed intrinsic microstresses σ_t . Thus the total stress is

$$\sigma = \sigma_a + \sigma_t, \quad (3.6)$$

where the perturbed stochastic component σ_t is of the same order as the applied stress field σ_a due to the microscale stress polarization (Section 4, Paper I) caused by differences in the elastic constants of mineral grains, and pore-space inhomogeneities. This stochastic component of stress supports critical crack distributions and plays a crucial role in the model proposed in Paper I, which displays effective anisotropy induced by applied stress σ_a only for physical processes effectively averaging the influence of microscale stochastic stress perturbations. We will show in the next section that propagating seismic waves effectively, and almost linearly, average the stress field through the interaction with crack distributions.

Another possibly observable consequence of fracture criticality is that there may be families of scale-invariant fractures

related to the crack clusters of different sizes. The proximity of crack density to fracture criticality and the percolation threshold suggests that crack clusters are likely to be distributed according to some scale-invariant power-law:

$$n(l)dl = Nl^{-x}dl, \quad (3.7)$$

where $n(l)dl$ is the volume concentration of crack clusters with characteristic size l , N is a normalizing factor and x is the exponent for the scale-invariant statistical parameters of the distribution of crack clusters. A simple but reasonable assumption that the total surface of crack clusters at different scales equals the total surface of individual microcracks allows us to estimate the statistical parameters N and x . We have

$$\int_a^\infty (\pi l^2)Nl^{-x}dl = \pi a^2 n_a = \pi \varepsilon / a, \quad (3.8)$$

where $n_a = \varepsilon a^{-3}$ is the volume concentration of microcracks. Integration of eq. (3.8) immediately gives values $N = \varepsilon$ and $x = -4$. The exponent $x = -4$ for a 3-D distribution (3.7) is consistent with the field observation of fracture distributions averaged over fracture lengths ranging from 10^{-5} to 10^5 m (Heffer & Bevan 1990).

Note that recognizing that scale-invariant distributions of fractures in crustal rocks are consistent with the idea of microcrack coalescence at different scales is not new (Allègre, Le Mouél & Provost 1982). Moreover, any direct application of the results of percolation theory to the problem of scale-invariant geological structures in crustal rocks, particularly in the form of oversimplified estimates as in (3.1) (3.3), and (3.8), must proceed with caution (Bebington, Vere-Jones & Zheng 1990; Heffer & Bevan 1990), and requires further investigation. Nevertheless, the existence of scale-invariant families of fractures caused by the critical nature of fluid-rock interaction at the grain-scales (the fracture criticality, or metastability, of the stressed fluid-saturated rock mass) with the parameter N of the order of the percolation threshold ε_p can be expected for all types of fluid-saturated polycrystalline rocks, even for ostensibly intact crustal rocks. In the general case of fractured crustal rocks with different geological histories, the microcrack-induced families of scale-invariant fractures can define the 'minimum' expected value of the scale-invariant fracture density N , of the order of the percolation threshold $\varepsilon_p \approx 0.1-0.2$, which seems to be consistent with the distribution of N reviewed by Heffer & Bevan (1990). In this case, the narrow range of observed stress-induced shear-wave velocity anisotropy, 1.5–4.5 per cent (Crampin 1994), is a further seismic demonstration of the self-organized criticality of crustal rocks (Turcotte 1992), which appears to be the result of the critical metastable nature of fluid-rock interaction at grain-scales in a pre-stressed fluid-saturated rock mass. Such plausible concepts have been demonstrated in several branches of physics, ranging from solid-state physics to global cosmology, where self-organized and self-similar macrostructures are a result of some critical physical or chemical microscale phenomenon (Ma 1976).

4 PHYSICAL REASONS FOR COUPLING BETWEEN DIFFERENTIAL STRESS AND SHEAR-WAVE SPLITTING

It has long been recognized theoretically (Nur 1971; Crampin 1978, 1981), experimentally (Nur & Simmons 1969), and in

field observations (Crampin *et al.* 1980, 1985) that the pervasive azimuthal shear-wave splitting observed in crustal rocks is a stress-induced phenomenon caused by stress-aligned fluid-filled EDA cracks (Crampin *et al.* 1984). However, the physical behaviour of cracked rock, and the physics of crack distributions responding to changes in the local and regional stress fields, has not previously been formulated theoretically. One of the barriers hindering such developments has been that in conventional poroelasticity theory (Biot 1941, 1956a,b) shear stresses are decoupled from pore fluid pressures so that the shear modulus and the velocities of shear waves are insensitive to pore fluid pressure and applied differential stress. In contrast, numerous laboratory experiments with pre-stressed cracked crystalline and sedimentary rocks (Nur & Simmons 1969; Sayers 1988; Rai & Hanson 1988; Siegesmund, Kern & Vollbrecht 1991; Sayers & van Munster 1991), and theoretical modelling (Nur 1971; Crampin 1978; Sayers 1988; amongst others), demonstrate that shear waves are very sensitive to modifications of pore space caused by differential stresses in the range 1–100 MPa.

The concept of fracture criticality, suggesting a narrow range of effective crack density for intact rock in the upper crust, appears to be in conflict with the idea of a close relationship between shear-wave splitting and varying stress field. The effects of eq. (3.5) demand changes in the effective crack density in response to small or moderate changes in differential components of the stress field expected before earthquakes. Moreover, the absence of significant variations in crack density before the 1986, $M=6$, North Palm Springs earthquake (Crampin *et al.* 1990) suggested that crack density remains a more-or-less constant, or at most, slowly increasing, function of increasing stress.

It was suggested (Peacock *et al.* 1988; Crampin *et al.* 1990, 1991) that the observed temporal variations in shear-wave splitting along ray-path directions close to the boundary of the shear-wave window quadrant perpendicular to the crack strike were caused by systematic changes in aspect ratio of the EDA crack distributions. Similar effects were modelled (Peacock *et al.* 1988; Crampin *et al.* 1990) by increasing the aspect ratio at a fixed crack density. The key question is whether an increase of pore fluid pressure caused by an increasing horizontal stress component, with subsequent micro-scale pore fluid diffusion, preferentially increases the crack aspect ratio or stimulates subcritical crack growth (Atkinson 1984), which would probably be indicated by an increase in the effective crack density. It is possible that both processes are important for the evolution of EDA crack distributions, but are likely to have very different characteristic times in response to the changes in stress field.

Since an increase of aspect ratio caused by differential dilatation of pore space is a poroelastic response to an increase of excess pore fluid pressure (Paper I), it seems likely that increases of aspect ratio would take precedence over subcritical crack growth for short-time changes in the stress field before earthquakes, with a possible slow further evolution due to the subcritical crack growth or other kinetic relaxation processes. Observations before and after the North Palm Springs earthquake agree with this interpretation (Crampin *et al.* 1990, 1991). The velocity of subcritical crack growth is directly proportional to the changes in differential stress components, and very slow velocities (10^{-11} m s $^{-1}$, Wilkins 1980) have been recorded in the laboratory for moderate values of

differential stress. However, kinetic effects need to be taken into account in self-consistent theoretical considerations. These problems will be investigated in further publications for different physical situations (changes in differential stress, overburden pressure, pore fluid pressure, and temperature and chemical activity of pore fluids, amongst others).

The crack distribution model developed in Paper I appears to provide a simple explanation for the specific change in shear-wave response to changes in the stress field before and after earthquakes. The elastic constants of pre-stressed fluid-saturated rocks for values of effective crack density $\varepsilon < 0.1$, which according to the fracture criticality concept can be considered as typical for almost all types of intact rocks in the upper crust (see Section 3), can be written (Paper I) as

$$C = C^s + \varepsilon \int \int_{\gamma \geq 0} R(\Omega) C^l(\gamma) d\Omega, \quad (4.1)$$

where C_{ijkl}^s is the tensor of elastic constants of uncracked solid, C_{ijkl}^l is the first-order correction for elastic constants of parallel cracks, R_{ijkl}^{pqrs} is the rotation matrix for fourth-order tensors (Paper I) and

$$\gamma = 1 + p_f/\sigma^c + \sigma_{ij} n_i n_j / \sigma^c = 1 + p + s_{ij} n_i n_j, \quad (4.2)$$

where excess pore fluid pressure p_f is a function of the differential component of the stress field σ_{ij} and is determined by an integral equation [eq. (3.24), Paper I], n_i is the i th component of the unit vector to the crack face and dimensionless p and s_{ij} are, respectively, p_f and σ_{ij} normalized by σ^c . In the simple model of equally sized microcrack distributions, γ can be considered as the normalized aspect ratio in the region of crack orientations where $g \geq 0$. In the general case of porous rocks, that is all rocks containing free fluids, γ specifies the differential dilation and closure of pore space. The main consequence of eq. (4.2) is that the variations of γ are related to the first-order variations of the stress field, since

$$d\gamma = n_i n_j (d\sigma_{ij}/\sigma^c) + (dp_f/d\sigma_{ij})(d\sigma_{ij}/\sigma^c). \quad (4.3)$$

The response of the elastic properties dC , and consequently the seismic-wave velocities, of the cracked rock to changes in the stress field is determined through the variational derivative of the elastic constants $dC/d\gamma$. We have

$$\begin{aligned} \delta C = (\delta C/d\gamma) \delta\gamma = \varepsilon \int \int_{\gamma + \delta\gamma \geq 0} R(\Omega) C^l(\gamma + \delta\gamma) d\Omega \\ - \varepsilon \int \int_{\gamma \geq 0} R(\Omega) C^l(\gamma) d\Omega, \end{aligned} \quad (4.4)$$

which can be expressed as

$$\delta C = \varepsilon \int \int_{\delta\gamma} R(\Omega) C^l(\gamma) d\Omega + \varepsilon \int \int_{\gamma \geq 0} R(\Omega) (\delta C^l/\delta\gamma) \delta\gamma d\Omega. \quad (4.5)$$

The first term in (4.5) corresponds to the variations in elastic constants due to changes in the distribution of crack orientations caused by the opening and closing of cracks at different orientations to the stress field by microscale fluid migration. The behaviour of shear waves due to such modifications of crack geometry was considered in Paper I for different physical situations. Note that because the value of the first term is proportional to the region of integration $\delta\gamma$, the elastic constants are approximately linearly dependent on $\delta\gamma$. Thus, $\delta\gamma \sim \delta\sigma_{ij}$ from (4.3), and the effect of stress-induced variations

to elastic properties, and consequently to velocities of seismic waves, is of first order in $\delta\sigma_{ij}/\sigma^c$.

The second term in eq. (4.5) corresponds to variations in the elastic constants caused by the changes in the geometry of individual cracks, or more generally by differential dilatation of pore space. As was shown in Paper I, the dependence of the first correction C_{ijkl}^l on the crack geometry and properties of fluid-filled cracks can be written as

$$C_{ijkl}^l \propto \mu \Lambda' \gamma r / (1 + \gamma r), \quad (4.6)$$

where $r = c_f \sigma^c = c_f/c_{cr}$ is the normalized dimensionless pore fluid compressibility c_f and $\Lambda' \sim 1$ is a dimensionless combination of Lamé constants, as in eq. (3.5). For normal fluids (fluids with the properties of water under near-surface conditions), r is about 10^{-3} – 10^{-2} for a critical stress σ^c in the range 1–10 MPa. This means that the effects of changes in stress on elastic properties caused by the second term in (4.5) are negligible in comparison with those of the first term.

However, for subcritical H_2O – CO_2 –salt pore fluid compositions under high pressure and temperature (Shmulovich, Tkachenko & Plyasunova 1995; Shmulovich & Graham 1996), the fluid compressibility c_f is high and r can be of order unity, so that the effect of crack dilatation due to the second term in eq. (4.5) is of the same first order of magnitude in relation to $\delta\sigma_{ij}/\sigma^c$ as the first term. This situation was discussed by Crampin *et al.* (1990), where pore fluid properties were estimated for high- P and $-T$ conditions at depth in the crust in order to explain the variations in shear-wave splitting observed before and after the North Palm Springs earthquake. The observations of shear-wave splitting showing such variations were from small earthquakes with depths from 12 to 20 km, with ray paths where pore fluid properties are expected to be substantially different from those at near-atmospheric conditions at the surface. The crack dilatation assumed by Peacock *et al.* (1988) and Crampin *et al.* (1990, 1991) is now shown to be a direct consequence of an increase in differential horizontal stress inducing pore fluid migration along pressure gradients between adjacent intergranular EDA microcracks at different orientations to the stress field.

The above discussion of the underlying physical mechanism for the stress-induced variations expected in the anisotropic behaviour of seismic waves is based on the general equation (4.5), and does not show how seismic waves will react to changes in the horizontal differential stress field. In the next section, we show that the principal effect of changes in differential stress is on ray paths close to the boundary of the shear-wave window in directions oblique to the average strike of the EDA cracks, in agreement with the interpretation of the observed variations before the 1986 North Palm Springs earthquake (Crampin *et al.* 1990).

It might be thought that the stochastic stress field discussed in the previous section may seriously affect the sensitivity of seismic waves to small variations in the average tectonic stress. The above discussion of the physical reasons for the coupling between shear waves and differential stress shows that this coupling is approximately linear over $\delta\sigma_{ij}/\sigma^c$. Thus the effective elastic constants given by eq. (4.1) are a result of linear averaging over crack distributions, at least for effective crack densities $\varepsilon \leq 0.1$. When cracks are distributed uniformly in space and consequently randomly affected by local stress perturbations (local stress polarizations) due to variations in grain lithology, pore shapes and other phenomena, variations

in seismic velocities will follow the average changes in the regional differential stress field where $\delta\gamma \sim \delta\sigma_{ij}/\sigma^c$ (eq. 4.3). The kinetic effects of crack growth and healing may disturb this simple coupling due to the changes in the effective crack density of the quasi-stationary crack distribution (this effect will be considered elsewhere), but nevertheless the conservation law for pore fluid and the concept of fracture criticality is likely to restrict possible changes in effective crack density.

5 MODELLING TEMPORAL VARIATIONS IN SHEAR-WAVE SPLITTING

The only existing observations of temporal changes in shear-wave splitting over a solid angle of directions wide enough for the changes to be quantified are temporal variations in the time delays between split shear waves reported before and after the 1986, $M=6$, North Palm Springs earthquake, Southern California (Crampin *et al.* 1990, 1991). [There have been a few reports of similar temporal variations before smaller earthquakes, consistent with the observations, but these have much less complete data sets (Booth *et al.* 1990; Liu *et al.* 1993; Gao *et al.* 1997) with much smaller coverage of the solid angle.] Station KNW, where the observations were made, is above a relatively simple geological structure characterized by a great thickness (approximately 21 km) of nearly constant P - and S -wave velocities (6.30 and 3.63 km s⁻¹, respectively; Hartzell & Brune 1979).

To model the seismic response to the possible changes in the differential component of (maximum) horizontal stress s_H , we have chosen a 3-D random distribution of cracks with an initial fixed value of crack density just below the percolation threshold pre-stressed by a fixed vertical differential stress $s_V = 20$ ($\Delta\sigma_V = \sigma_V - \sigma_h = 20\sigma^c$ for dimensional differential stress). Note that $\Delta\sigma_V$ is the difference between the vertical and least horizontal components of stress, and at depth is much less than the lithostatic (overburden) pressure. In this case, the model developed in Paper I is entirely constrained and has no free parameters. The seismic response of rock with fluid-saturated intergranular EDA cracks depends only on the relationship between the dimensionless differential components of the stress field. The insensitivity of the subcritical crack distribution to the value of the differential vertical stress demonstrates that the observed effects imply variations in horizontal differential stress. Fig. 4 shows the evolution of split shear waves in initially randomly oriented vertical cracks under increasing s_H in the range $s_H=0$ to $s_H=10$, for $s_H \leq s_V/2$, where $s_V=20$ and $s_h=0$. The dashed lines correspond to observations of shear-wave splitting inferred from the seismic data (Peacock *et al.* 1988; Crampin *et al.* 1990, 1991) for average stress conditions, and we see that from an initially random distribution of nearly vertical cracks the shear-wave splitting becomes close to the behaviour observed at Anza. Note that the 3-D pattern of stress-induced variations in the region of the shear-wave window (effectively 45° from the vertical) is similar to that which was initially proposed to explain the observations by Peacock *et al.* (1988) and Crampin *et al.* (1990, 1991).

Fig. 5(a) shows a simple stress-time history used to model the smoothly increasing maximum horizontal stress before an earthquake. The sequence begins with a linear build-up to a maximum value of differential horizontal stress $s_H - s_h = 10$, and an abrupt decrease at the time of (or in one case shortly

before, Booth *et al.* 1990) the main shock. The lithostatic (vertical) overburden stress and minimum horizontal stress are assumed to be constant during the earthquake cycle.

It was recognized by Peacock *et al.* (1988) and Crampin *et al.* (1990, 1991) that, in the stress conditions at Anza, time delays are most sensitive to stress variations for ray-path directions to the surface between about 45° and 75° to the crack plane, in the quadrant of azimuths bisected by the s_h to s_V plane. The difference between the split shear waves in these directions, proportional to the time delay, is the solid area in the top two diagrams of Fig. 4 for $s_H=7$ and $s_H=10$. The ratio between the solid area and the open area at less than 15° to the crack plane is greater for $s_H=10$ than for $s_H=7$. Fig. 5(b) shows observed time delays (stars) for angles between 45° and 75° to the vertical above small earthquakes in the specific azimuthal quadrant before and after the North Palm Springs earthquake (Crampin *et al.* 1990). The lines are average values of calculated time delays for ray-path directions between 45° and 75° in the azimuthal quadrant for the simple stress history in Fig. 5(a) of a linear increase and an abrupt decrease in s_H at the time of the earthquake. The solid line corresponds to a pore fluid with the compressibility of water at atmospheric temperatures and pressures. As the earthquakes were comparatively deep, approximately 20 km, the dashed line is the expected effect of cracks filled with a fluid composition H₂O-CO₂-salt at temperatures and pressures appropriate to about 10 km depth (Shmulovich *et al.* 1995; Shmulovich & Graham 1996), approximately halfway along the ray paths. The dashed line is a good fit to the observations.

6 DISCUSSION

Numerical APE modelling of rock-mass deformation matches observations for a wide range of different phenomena, as listed below:

- (1) APE modelling matches the minimum shear-wave velocity anisotropy in intact rock below 1 km depth (observed 1.5 per cent; modelled 1 per cent);
- (2) APE matches the upper fracture-criticality limit of shear-wave velocity anisotropy in intact rock below 1 km depth (observed 4.5 per cent; modelled 5 per cent);
- (3) APE matches the evolution of microcracked rock in a crustal stress field in Fig. 4;
- (4) there is compatibility between the fracture criticality (percolation threshold) and the observed scale-invariant distributions of fractures over 10 orders of magnitude;
- (5) APE modelling matches the observed variations in shear-wave splitting observed before and after the North Palm Springs earthquake in Fig. 5 (and several smaller earthquakes elsewhere) for a simple increase of differential horizontal stress.

What is particularly surprising is that the microscale APE modelling matches macroscale observations of shear-wave splitting despite the evident heterogeneities throughout all crustal rocks. Occam's razor suggests that APE modelling is at least a good first-order approximation to the numerical equation of state for the behaviour of a pre-stressed fluid-saturated rock mass.

APE has several first-order implications. Microscale fluid flow between adjacent intergranular microcracks and pores largely controls small-scale deformation of *in situ* rock, which is dominated by pore fluid migration. The immediate effect is

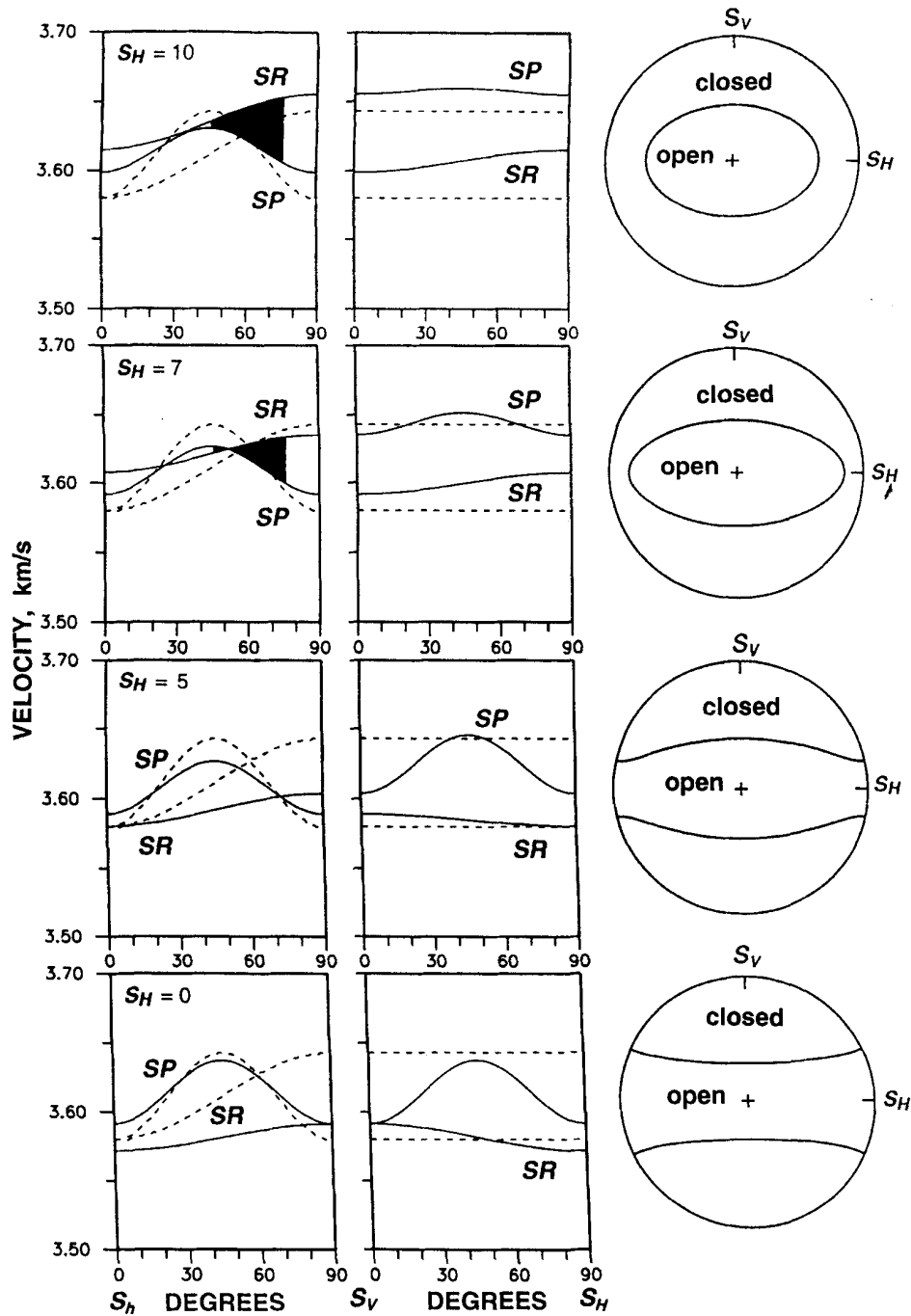


Figure 4. Left-hand and centre diagrams: evolution of shear-wave velocities showing two approximately orthogonally polarized shear waves. Solid lines: effects of increasing horizontal differential stress from bottom $s_H=0$ ($s_H=s_h$), 5, 7 and 10, for $s_V=20$ and $s_h=0$. Dashed lines: velocities inferred from Anza (Crampin *et al.* 1990) for a fixed model of parallel vertical EDA cracks. Velocities of the two split shear waves are shown in two orthogonal planes of symmetry s_h (0°) to s_V (90°), and s_V (0°) to s_H (90°), where SP is polarized parallel and SR at right-angles to each plane of variation. The solid areas in the top two diagrams at angles of incidence between 15° and 45° in the s_V - s_h are proportional to the time delays along ray paths in these directions plotted in the lower diagram in Fig. 5. Right-hand diagrams: equal-area polar plots about the s_h direction of the line marking the boundary of the distribution of closed cracks.

to redistribute pore fluids between neighbouring microcracks and pores by modifying effective aspect ratios at different orientations to the stress field. The widely observed shear-wave splitting in the crust (Crampin 1994) means that the frequently neglected differential horizontal stress is typically

sufficient to align the microstructure of rocks in the crust. These microscales are the smallest elements of self-similar structures controlling macroscale observations including distributions of fractures and macroscopic observations of shear waves (suggesting that the observational seismic gap between

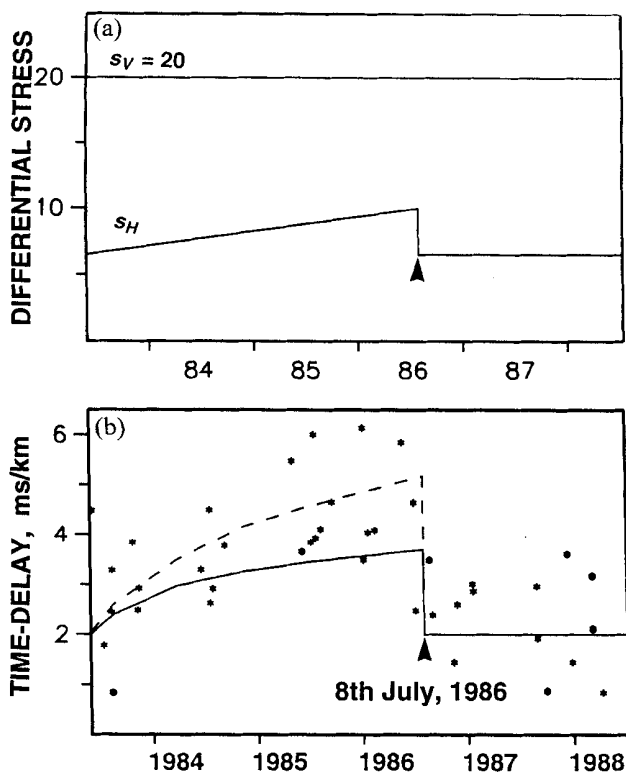


Figure 5. Upper diagram: possible time history of horizontal differential stress component s_H in an earthquake cycle in the presence of a larger vertical differential stress s_V . The horizontal begins at an initial level $s_H = 7$, increases linearly to $s_H = 10$, and then decreases abruptly near the time of the earthquake. The arrowhead marks the time of the hypothetical earthquake. Lower diagram: Variations in time delays in shear-wave splitting for ray-path directions between 45° and 75° to the crack plane in the azimuthal quadrant bisecting the direction normal to the crack plane before and after the North Palm Springs earthquake. The solid line corresponds to the pore fluid with compressibility of water at atmospheric temperatures and pressures for the stress history in the upper diagram. The dashed line is the expected effect of cracks filled with H_2O-CO_2 -salt pore fluid compositions at temperatures and pressures appropriate to about 10 km depth (Shmulovich *et al.* 1995; Shmulovich & Graham 1996), approximately halfway along the ray paths. Observations (stars) are taken from Fig. 3(d) of Crampin *et al.* (1990). The arrowhead marks the time of the North Palm Springs earthquake.

P-wave observations at frequencies between 1 kHz and 30 Hz, say, is at least partially transparent to shear waves). The similarity between the modelled and observed behaviour before earthquakes suggests that at least some earthquakes are the result of comparatively simple increases in differential horizontal stress, and that these changes can be monitored by appropriate observations of shear waves. One of the most important implications is that *microscale* behaviour can be monitored with observations of *macroscale* shear-wave splitting.

These implications are not exhaustive. The developments lead, we suggest, to a new understanding of the behaviour of all rocks containing free fluids and there may well be other important implications and applications that are not yet obvious.

What is not understood at present is the effect of frequency

and spatial dispersion of seismic waves in fluid-saturated porous rocks (Dvorkin & Nur 1993; Hudson, Liu & Crampin 1996). The approximation used in this paper and Paper I is a simple low-frequency calculation of the variations in seismic wave velocities due to an applied stress field. We have demonstrated that the anisotropic stress-induced crack distribution is supported by intrinsic microstresses and, because of the various stress-relaxation mechanisms modifying the internal crack and pore geometry, is in a *metastable* condition. Consequently, *kinetic* stress-relaxation processes will also affect the evolution of quasi-stationary crack distributions in fluid-saturated crustal rocks. These processes include subcritical crack growth, crack healing, intracrystalline plasticity and chemical fluid-rock interactions, amongst others. As we argued in Paper I and in Section 3 of this paper, full relaxation of intrinsic microstresses in continuously deformed pre-stressed fluid-saturated rock is impossible. At microscale level there will always exist perturbed stochastic stress components of the same order as the average (applied) differential stresses caused by differences in the elastic constants of different mineral grains, and by pore-space inhomogeneities. These stochastic stress components support metastable quasi-stationary crack distributions with parameters defined by the average (applied) differential stress. The anisotropic quasi-stationary EDA crack distributions satisfy the microscale stress balance between the average stress field with deviatoric components and the essentially isotropic pore fluid pressure (Paper I). We have demonstrated that such crack distributions are sensitive to even small changes in the stress conditions of fluid-saturated crustal rocks.

7 CONCLUSIONS

We conclude that stress-induced variations in shear-wave splitting in ostensibly intact rocks in at least the upper 15 km of the crust is controlled by pressure-induced pore fluid migration at the microscale level, leading to the stress sensitivity and compliance of fluid-saturated crustal rocks. We have demonstrated that the narrow range of observed stress-induced anisotropy, 1.5–4.5 per cent, can be interpreted as confirmation of the self-organized criticality of crustal rocks at the fundamental grain-scale level and the proximity of fracture criticality in all fluid-saturated crustal rock. Theoretical modelling of the stress-sensitive behaviour of split shear waves develops the concept of extensive-dilatancy anisotropy (EDA), where the fluid-rock interaction and pore fluid dynamics at the grain-scale level are an integral part of the analysis. The qualitative and quantitative agreement of theoretical results of microscale modelling and field observations of macroscale seismic wavelengths is remarkable and suggests that both the modelling and the interpretation of the observations are good first-order approximations to fluid-rock interactions in *in situ* rock. We have shown that much of the behaviour of fluid-saturated stress-sensitive rock is essentially controlled by the frequently neglected differential horizontal components of the *in situ* stress field. Consequently, any analysis which neglects differential horizontal stress in the stress state of crustal rock is at best incomplete, and at worse may introduce serious errors into estimates of fluid-rock interactions.

This analysis also suggests that the microscale structure of rock is sensitive to even small changes in the differential horizontal stress field due to the proximity of metastability and fracture criticality. Further, it suggests that such small

changes in stress can be monitored by corresponding changes in the behaviour of seismic shear waves. Since the stress state of rock mass directly or indirectly depends on local and tectonic stresses, pore fluid pressure, temperature, composition and chemical activity, amongst others, this means that shear waves are also sensitive to variations in all these parameters and can be used to monitor the deformation of the stress-sensitive fluid-saturated rock mass.

ACKNOWLEDGMENTS

The authors thank Peide Wang for showing them the Hainan Island aftershock data before publication, and Peter C. Leary, Kes J. Heffer and Kirill I. Shmulovich for invaluable comments and discussion throughout this research. SVZ was partially supported by a fellowship from the Royal Society and by British Petroleum. SC was partially supported by the Natural Environment Research Council.

REFERENCES

- Aggarwal, Y.P., Sykes, L.R., Armbruster, J. & Sbar, M.L. 1973. Premonitory changes in seismic velocities and prediction of earthquakes, *Nature*, **241**, 101–104.
- Aggarwal, Y.P., Sykes, L.R., Simpson, D.W. & Richards, P.G., 1975. Spatial and temporal variations in t_s/t_p and in the P -wave residuals at Blue Mountain Lake, New York: application to earthquake prediction, *J. geophys. Res.*, **80**, 718–732.
- Alford, R.M., 1986. Shear data in the presence of azimuthal anisotropy: Dilley, Texas, 56th Ann. Int. SEG Meeting, Houston. Expanded Abstracts, 476–479.
- Allègre, C.J., Le Mouel, J.L. & Provost, A., 1982. Scaling rules in rock fracture and possible implications for earthquake prediction, *Nature*, **297**, 47–49.
- Aster, R.C., Shearer, P.M. & Berger, J., 1990. Quantitative measurements of shear-wave polarizations at the Anza seismic network, Southern California: implications for shear-wave splitting and earthquake prediction, *J. geophys. Res.*, **95**, 12449–12473.
- Aster, R.C., Shearer, P.M. & Berger, J., 1991. Reply to Crampin *et al.* (1991), *J. geophys. Res.*, **96**, 6415–6419.
- Atkinson, B.K., 1984. Sub-critical crack growth in geological materials, *J. geophys. Res.*, **89**, 4077–4114.
- Bebbington, M., Vere-Jones, D. & Zheng, X., 1990. Percolation Theory: a model for rock fracture?, *Geophys. J. Int.*, **100**, 215–220.
- Biot, M.A., 1941. General theory of three-dimensional consolidation, *J. appl. Phys.*, **12**, 155–164.
- Biot, M.A., 1956a. Theory of propagation of elastic waves in a fluid saturated porous solid. I. Low-frequency range, *J. acoust. Soc. Am.*, **28**, 168–178.
- Biot, M.A., 1956b. Theory of propagation in a fluid saturated porous solid. II. Higher-frequency range, *J. acoust. Soc. Am.*, **28**, 179–191.
- Booth, D.C. & Crampin, S., 1985. Shear-wave polarizations on a curved wavefront at an isotropic free-surface, *Geophys. J. R. astr. Soc.*, **83**, 31–45.
- Booth, D.C., Crampin, S., Lovell, J.H. & Chiu, J.-M., 1990. Temporal changes in shear wave splitting during an earthquake swarm in Arkansas, *J. geophys. Res.*, **95**, 11 151–11 164.
- Brodie, K.H. & Rutter, E.H., 1985. On the relationship between deformation and metamorphism, with special reference to the behaviour of basic rock, in *Metamorphic Reactions: Kinetics, Textures, and Deformation*, eds Thompson, A.B. & Rubie, D.C., *Advances in Physical Geochemistry*, **4**, 138–179, Springer-Verlag, New York, NY.
- Byerly, P., 1938. The earthquake of July 6, 1934; amplitudes and first motions, *Bull. seism. Soc. Am.*, **28**, 1–13.
- Chelidze, T., 1982. Percolation and fracture, *Phys. Earth planet. Inter.*, **28**, 93–101.
- Chelidze, T., 1986. Percolation theory as a tool for imitation of fracture processes in rocks, *Pure. appl. Geophys.*, **124**, 731–748.
- Chiu, J.-M., Johnston, A.C., Metzger, A.G., Haar, L. & Fletcher, J., 1984. Analysis of analog and digital records of the 1982 Arkansas earthquake swarm, *Bull. seism. Soc. Am.*, **74**, 1721–1742.
- Crampin, S., 1978. Seismic wave propagation through a cracked solid: polarization as a possible dilatancy diagnostic, *Geophys. J. R. astr. Soc.*, **53**, 467–496.
- Crampin, S., 1981. A review of wave motion in anisotropic and cracked elastic-media, *Wave Motion*, **3**, 343–391.
- Crampin, S., 1984a. Anisotropy in exploration seismics, *First Break*, **2** (3), 19–21.
- Crampin, S., 1984b. Effective anisotropic elastic-constants for wave propagation through cracked solids, *Geophys. J. R. astr. Soc.*, **76**, 135–145.
- Crampin, S., 1987. Geological and industrial implications of extensive-dilatancy anisotropy, *Nature*, **328**, 491–496.
- Crampin, S., 1989. Suggestions for a consistent terminology for seismic anisotropy, *Geophys. Prospect.*, **37**, 753–770.
- Crampin, S., 1991. An alternative scenario for earthquake prediction experiments, *Geophys. J. Int.*, **107**, 185–189.
- Crampin, S., 1993. Do you know of an isolated swarm of small earthquakes? *EOS, Trans. Am. geophys. Un.*, **74**, 451 & 460.
- Crampin, S., 1994. The fracture criticality of crustal rock, *Geophys. J. Int.*, **118**, 428–438.
- Crampin, S. & Booth, D.C., 1989. Shear-wave splitting showing hydraulic dilatation of pre-existing joints in granite, *Sci. Drilling*, **1**, 21–26.
- Crampin, S., Evans, R., Üçer, B., Doyle, M., Davis, J.P., Yegorkina, G.V. & Miller, A., 1980. Observations of dilatancy-induced polarization anomalies and earthquake prediction, *Nature*, **286**, 874–877.
- Crampin, S., Evans, R., Doyle, M. & Davis, J.P., 1981. Comments on papers about shear-wave splitting in dilatancy-induced anisotropy by I.N. Gupta and by A. Ryall & W.U. Savage, *Bull. seism. Soc. Am.*, **71**, 375–377.
- Crampin, S., Evans, R. & Atkinson, B.K., 1984. Earthquake prediction: a new physical basis, *Geophys. J. R. astr. Soc.*, **76**, 147–156.
- Crampin, S., Evans, R. & Üçer, S.B., 1985. Analysis of records of local earthquakes: the Turkish Dilatancy Projects (TDP1 and TDP2), *Geophys. J. R. astr. Soc.*, **83**, 1–16 & 17–92.
- Crampin, S., Bush, I., Naville, C. & Taylor, D.B., 1986. Estimating the internal structure of reservoirs with shear-wave VSPs, *The Leading Edge*, **5** (11), 35–39.
- Crampin, S., Booth, D.C., Evans, R., Peacock, S. & Fletcher, J.B., 1990. Changes in shear-wave splitting at Anza near the time of the North Palm Springs Earthquake, *J. geophys. Res.*, **95**, 11 197–11 212.
- Crampin, S., Booth, D.C., Evans, R., Peacock, S. & Fletcher, J.B., 1991. Comment on 'Quantitative measurements of shear wave polarizations at the Anza Seismic Network, Southern California: implications for shear wave splitting and earthquake prediction' by R.C. Aster, P.M. Shearer & J. Berger, *J. geophys. Res.*, **96**, 6403–6414.
- Dienes, J.K., 1982. Permeability, percolation, and statistical crack mechanics, *Proc. 23rd US Symp. Rock Mechanics, Berkeley, CA*, 96–94.
- Dvorkin, J. & Nur, A., 1993. Dynamic poroelasticity: A unified model with the squirt and Biot mechanisms, *Geophysics*, **58**, 524–533.
- Evans, R., Beamish, D., Crampin, S. & Üçer, S.B., 1987. The Turkish Dilatancy Project (TDP3): multidisciplinary studies of a potential earthquake source region, *Geophys. J. R. astr. Soc.*, **91**, 265–286 & 287–330.
- Fyfe, W.S., Price, N.J. & Thompson, A.B., 1978. *Fluids in the Earth's Crust, Developments in Geochemistry*, **1**, Elsevier, Amsterdam.
- Gao, Y., Wang, P., Zheng, S., Wang, M. & Chen, Y.-T., 1997. Temporal changes in shear-wave splitting at an isolated swarm of small earthquakes in 1992 near Dongfang, Hainan Island, Southern China, *Geophys. J. Int.*, submitted.
- Géraud, Y., 1994. Variations in connected porosity and inferred

- permeability in a thermally cracked granite, *Geophys. Res. Lett.*, **21**, 979–982.
- Gueguen, Y. & Dienes, J.K., 1989. Transport properties of rocks from statistics and percolation, *J. int. Assoc. math. Geol.*, **21**, 1–13.
- Gupta, I.N., 1973. Premonitory variations in *S*-wave velocity anisotropy before earthquakes in Nevada, *Science*, **182**, 1129–1132.
- Hartzel, S.H. & Brune, J.N., 1979. The Horse Canyon earthquake of August 2, 1975 – two-stage stress-release process in a strike-slip earthquake, *Bull. seism. Soc. Am.*, **69**, 1161–1174.
- Heffer, K.J. & Bevan, T.G., 1990. Scaling relationships in natural fractures: data, theory, and applications, *Proc. Europec'90, SPE Paper 20981*, 367–376.
- Hudson, J.A., 1981. Wave speeds and attenuation of elastic waves in material containing cracks, *Geophys. J. R. astr. Soc.*, **64**, 133–150.
- Hudson, J.A., Liu, E. & Crampin, S., 1996. The mechanical properties of materials with interconnected cracks and pores, *Geophys. J. Int.*, **124**, 105–112.
- Kirkpatrick, S., 1973. Percolation and conduction, *Rev. mod. Phys.*, **45**, 574–588.
- Kranz, R.L., 1983. Microcracks in rocks: a review, *Tectonophysics*, **100**, 449–480.
- Lee, C.-H. & Farmer, I., 1993. *Fluid Flow in Discontinuous Rocks*, Chapman & Hall, London.
- Liu, E., Crampin, S. & Hudson, J.A., 1995. Diffraction of seismic waves by cracks with application to hydraulic fracturing, *Geophysics*, **62**, 253–265.
- Liu, Y., 1995. Shear-wave anisotropy and the interpretation of temporal changes in time delays, *PhD thesis*, University of Edinburgh.
- Liu, Y., Booth, D.C., Crampin, S., Evans, R. & Leary, P., 1993. Shear-wave polarizations and possible temporal variations in shear-wave splitting at Parkfield, *Can. J. expl. Geophys.*, **29**, 380–390.
- Ma, S., 1976. *Modern Theory of Critical Phenomena*, *Frontiers in Physics*, Benjamin-Cummings, Reading, MA.
- Meadows, M.A. & Winterstein, D.L., 1994. Seismic detection of a hydraulic fracture from shear-wave VSP data at Lost Hills field, California, *Geophysics*, **57**, 11–26.
- Neuzil, C.E., 1995. Abnormal pressures as hydrodynamic phenomena, *Am. J. Sci.*, **295**, 742–786.
- Nur, A., 1971. Effects of stress on velocity anisotropy in rocks with cracks, *J. geophys. Res.*, **76**, 2022–2034.
- Nur, A., 1972. Dilatancy, pore fluids, and premonitory variations of travel times, *Bull. seism. Soc. Am.*, **78**, 1217–1222.
- Nur, A. & Simmons, G., 1969. Stress-induced velocity anisotropy in rock: an experimental study, *J. geophys. Res.*, **74**, 6667–6674.
- Peacock, S., Crampin, S., Booth, D.C. & Fletcher, J.B., 1988. Shear-wave splitting in the Anza seismic gap, Southern California, temporal variations as possible precursors, *J. geophys. Res.*, **93**, 3339–3356.
- Rai, C.S. & Hanson, K.E., 1988. Shear-wave velocity anisotropy in sedimentary rocks: a laboratory study, *Geophysics*, **23**, 800–806.
- Sayers, C.M., 1988. Stress-induced ultrasonic wave velocity anisotropy in fractured rock, *Ultrasonics*, **26**, 311–317.
- Sayers, C.M. & van Munster, J.G., 1991. Microcrack-induced seismic anisotropy of sedimentary rocks, *J. geophys. Res.*, **96**, 16 529–16 533.
- Semenov, A.N., 1969. Variations in the travel time of transverse and longitudinal waves before violent earthquakes, *Izv. acad., Sci. USSR Phys. solid Earth*, **4**, 245–248, English translation.
- Shakespeare, W., 1623. *Macbeth*, 1623 Folio.
- Shmulovich, K.I. & Graham, C.M., 1996. Melting of albite and dehydration of brucite in H₂O–NaCl fluids to 9 kbars and 700–900 °C: implications for partial melting and water activities during high pressure metamorphism, *Contrib. Mineral. Petrology*, **124**, 370–382.
- Shmulovich, K.I., Tkachenko, S.I. & Plyasunova, N.V., 1995. Phase equilibria in fluid systems at high pressures and temperatures, in *Fluids in the Crust. Equilibrium and Transport Properties*, pp. 193–212, eds Shmulovich, K.I., Yardley, B.W.D. & Gonchar, G.G., Chapman & Hall, London.
- Siegesmund, S., Kern, H. & Vollbrecht, A., 1991. The effect of oriented microcracks on seismic velocities in an ultramylonite, *Tectonophysics*, **186**, 241–251.
- Simmons, G. & Richter, D., 1976. Microcracks in rocks, in *Physics and Chemistry of Minerals and Rocks*, pp. 105–137, ed. Strens, R.G.J., John Wiley & Sons, New York, NY.
- Turcotte, D.L., 1992. Fractals, chaos, self-organized criticality and tectonics, *Terra Nova*, **4**, 4–12.
- Whitcomb, J.H., Garmany, J.D. & Anderson, D.L., 1973. Earthquake prediction: variation of seismic velocities before the San Fernando earthquake, *Science*, **180**, 632–635.
- Wilkins, J.S., 1980. Slow crack growth and delayed failure of granite, *Int. J. Rock Mech. Min. Sci.*, **17**, 365–369.
- Willis, H.A., Rethford, G.L. & Bielandski, E., 1986. Azimuthal anisotropy: occurrence and effect on shear-wave data quality, *56th Ann. Int. SEG Meeting, Houston, Expanded Abstracts*, 479–481.
- Zatsepin, S.V. & Crampin, S., 1997. Modelling the compliance of crustal rock—I. Response of shear-wave splitting to differential stress, *Geophys. J. Int.*, **129**, 477–494 (this issue).